Proceedings of CONF-FMCE 2025 Symposium: Semantic Communication for Media Compression and Transmission
DOI: 10.54254/2755-2721/2025.GL27816

Remote Sensing–Based Quantification of Shanghai's Summer Urban Heat-Island Intensity and NDVI

Chaohan Zhou

Department of Earth Science, University College London, London, United Kingdom
zcfbcz2@ucl.ac.uk

Abstract. Urban heat island (UHI) elevates land surface temperature (LST) and stresses public health and energy systems. Urban vegetation can lower LST through shading and evapotranspiration, yet practical guidance on how much greening is needed and where to prioritize it remains limited. Focusing on highly urbanized Shanghai, we used Google Earth Engine to integrate Sentinel-2 NDVI with Landsat 8/9 LST and computed district-level summer (June–August 2022) means of NDVI, LST, and surface UHI (SUHI). We assessed vegetation–temperature relationships using Pearson correlation and ordinary least squares. NDVI and LST were strongly and significantly negatively correlated ($r \approx -0.73$, $p < 0.05$); districts with higher vegetation cover showed lower LST and weaker UHI. The regression slope indicates that a 0.1 increase in NDVI is associated with ~2.4 °C lower district-mean LST. Based on current land-use patterns, we mapped zones with the greatest greening-for-cooling potential to inform zoning-specific strategies. The results provide quantitative evidence that expanding urban green space is an effective pathway to mitigate UHI and enhance climate resilience and public well-being in megacities.

Keywords: NDVI, Land surface temperature, Urban heat island.

1. Introduction

Urbanization is advancing at an unprecedented pace, continuously altering land cover, energy use, and the urban surface–atmosphere energy balance. One of its most salient by-products is the surface urban heat island (SUHI) effect: extensive impervious surfaces absorb and re-radiate heat, causing urban land surface temperature (LST) to exceed that of surrounding rural areas by several degrees Celsius [1]. Elevated LST not only intensifies human heat stress and electricity demand, but also promotes near-surface ozone formation via photochemical reactions, posing risks to public health [2]. By contrast, urban vegetation can effectively reduce near-surface temperature through shading and evapotranspiration [3] and can increase surface roughness to enhance turbulent heat dissipation [4]. Consequently, determining how much greening is needed and where it should be prioritized remains a critical question for climate-adaptive urban planning.

Remote sensing offers an efficient, economical, and repeatable means of examining these processes. The normalized difference vegetation index (NDVI), which exploits reflectance contrasts between the red and near-infrared bands, has become the most widely used indicator of vegetation cover and health [5]. Thermal-infrared imagery enables pixel-scale retrieval of land surface

© 2025 The Authors. This is an open access article distributed under the terms of the Creative Commons Attribution License 4.0 (https://creativecommons.org/licenses/by/4.0/).

DOI: 10.54254/2755-2721/2025.GL27816

temperature, allowing a single satellite overpass to characterize city-wide SUHI intensity patterns [6]. Compared with traditional ground observations that rely on sparse stations and are labor-intensive, satellite-based metrics capture intra-urban temperature heterogeneity, temporal dynamics, and cross-scale interactions at lower cost [7].

However, many existing studies tend to focus on only one facet—either vegetation or the thermal environment. High-resolution imagery excels at extracting urban green spaces and monitoring greening rates, where finer spatial detail helps reduce land-cover misclassification and improve management decisions [8]; land-use studies, in turn, reveal the expansion of impervious surfaces and the loss of agricultural land, illustrating how spatial competition among uses shapes urban microclimates [9]. These strands are rarely integrated to uncover the spatial coupling and feedback between vegetation and heat. Moreover, classification approaches—from visual interpretation to machine learning—vary in efficiency, accuracy, and scalability, hindering cross-study comparability and complicating evidence-based setting of greening thresholds.

To bridge these gaps, we built a cloud-native workflow on the Google Earth Engine (GEE) platform that integrates Sentinel-2-derived NDVI with Landsat-8/9-derived LST. We first extracted district-level averages of LST and SUHI for Shanghai according to administrative/functional zoning, and concurrently derived co-period NDVI to characterize the green-space pattern. We then employed correlation analysis, geographically weighted regression (GWR), and hotspot analysis to evaluate the spatial coupling between vegetation and the UHI, identifying areas where vegetation exerts the strongest cooling effect. We further tested linear and nonlinear models to quantify the marginal cooling benefits of increasing NDVI, finding that the cooling effect tends to saturate at higher NDVI levels [10]. Under current land-use constraints, we delineated priority intervention areas with the greatest greening-for-cooling potential.

This study contributes in three ways: (1) it develops an open and reproducible spatiotemporal database of SUHI–NDVI, enabling automated processing and long-term monitoring of multi-source remote-sensing data without reliance on proprietary software; (2) it adopts a zoning-based analytical framework aligned with municipal planning units, allowing biophysical findings to be translated directly into guidance on greening quotas, land-use zoning, and climate-resilience targets; and (3) it compares areas with differing socioeconomic and morphological characteristics, providing quantitative evidence for the equitable and efficient allocation of urban green infrastructure. Ultimately, we aim to answer the core question of where, and by how much, vegetation can deliver effective cooling, thereby furnishing robust scientific support for urban greening decisions that balance ecological integrity, human well-being, and sustainable development.

2. Data and methods

2.1. Study area

Shanghai is located at the Yangtze River estuary in eastern China, approximately between 30°40′–31°53′N and 120°52′–122°12′E. The municipal land area is about 6,340.5 km². The terrain is flat, and the climate is subtropical monsoon with four distinct seasons; summers are hot and humid, with frequent sultry weather in July–August each year. This study takes the administrative area of Shanghai as the analysis extent and selects the summer of 2022 (June 1–August 31) as the study period. During this period, vegetation is vigorous, precipitation is relatively concentrated, and land surface temperature (LST) is high, which is conducive to revealing the relationship between the distribution of urban green spaces and the surface thermal environment.

DOI: 10.54254/2755-2721/2025.GL27816

2.2. Data sources

All data acquisition and processing were conducted on the Google Earth Engine (GEE) cloud platform. The main data sources include:

(1) Landsat 8/9 OLI–TIRS Collection 2 Level 2: Level 2 imagery from the U.S. Landsat 8 and 9 satellites, providing atmospherically corrected surface reflectance and thermal infrared (TIR) bands. The visible and near-infrared (VNIR) bands have a spatial resolution of 30 m; the native TIR resolution is 100 m (resampled by the product to 30 m). Multi-temporal scenes covering Shanghai during the study period were used for land surface temperature (LST) retrieval.

(2) Sentinel-2 MSI Level 2A: Level-2A imagery from ESA's Sentinel-2 multispectral instrument, providing atmospherically corrected surface reflectance. The red band (~0.665 μm) and near-infrared band (~0.842 μm) have 10 m resolution. Multi-temporal Sentinel-2 images in summer 2022 were used to compute the normalized difference vegetation index (NDVI).

(3) Administrative boundaries of Shanghai: Polygon vector data for the municipal boundary and district boundaries, obtained from municipal open data. These data were used to clip the remote-sensing imagery to the study area and to provide spatial units for subsequent district-level statistics.

2.3. Data preprocessing

A unified preprocessing workflow was applied to the above remote-sensing data, with the main steps as follows:

(1) Cloud and shadow masking: We used quality-control information embedded in the imagery to identify and remove cloud and cloud-shadow pixels. Specifically, for Landsat 8/9 Level 2 imagery, the QA_PIXEL bitmask was used to filter out fill values, clouds, cirrus, and cloud shadows. For Sentinel-2, a cloud mask was applied to remove cloud-affected pixels. Only clear-sky pixels were retained for subsequent analysis.

(2) Atmospheric correction: The Landsat 8/9 and Sentinel-2 Level 2 products used here are already atmospherically corrected, providing surface reflectance and surface brightness temperature, so no additional atmospheric correction was performed. During preprocessing, Landsat radiometric scaling factors and temperature conversion were applied to convert TIR data to physical temperature (Kelvin), and then 273.15 was subtracted to obtain degrees Celsius. Sentinel-2 Level-2A data were directly used for NDVI calculation.

(3) Median compositing: To obtain representative imagery for the study period, multi-temporal images were composited using the per-pixel median. On GEE, we assembled all valid Landsat 8/9 scenes and Sentinel-2 scenes from June–August 2022 and computed median values for each band to generate summer composites of LST and NDVI. Median compositing reduces the impact of outliers (e.g., residual cloud noise or transient temperature fluctuations) and better represents average conditions over the period.

(4) Projection and resolution harmonization: The Sentinel-2-derived NDVI was resampled to 30 m to match the spatial resolution of Landsat LST. Bilinear interpolation was used to preserve NDVI spatial patterns as far as possible. All data were aligned on a common WGS-84 geographic grid to ensure pixel-level co-registration across sources.

(5) Study-area clipping: Using the Shanghai administrative boundary, the summer LST and NDVI composites were clipped to the municipal extent, yielding base rasters for subsequent analysis.

DOI: 10.54254/2755-2721/2025.GL27816

2.4. Index calculation

Land Surface Temperature (LST) retrieval: We applied the single-channel (single-window) algorithm to retrieve LST from Landsat 8/9 TIR imagery [11]. The method estimates LST by establishing an empirical linear relationship between satellite brightness temperature in a single TIR band and actual LST. We first computed brightness temperature from the TIR band, then performed atmospheric adjustments using parameters such as atmospheric transmittance and mean atmospheric temperature, and finally solved for LST. Surface emissivity effects were considered by estimating pixel-wise emissivity from NDVI: pixels with higher vegetation cover were assigned higher emissivity, whereas bare soil or built-up pixels with low vegetation cover were assigned lower emissivity. Emissivity estimation was interpolated from vegetation cover inferred by NDVI to ensure retrieval accuracy. Substituting these parameters into the single-channel equations produced LST maps for each pixel in Shanghai during the study period. In code implementation, we also validated the reliability of the LST retrievals using the single-channel framework.

This study computes NDVI using Sentinel-2 Level-2A imagery, specifically the red band (B4; center wavelength ~665 nm) and near-infrared band (B8; center wavelength ~842 nm). First, the red and near-infrared reflectance values of each image pixel are substituted into the above formula to obtain the pixel-level NDVI. NDVI ranges from −1 to 1, with higher values indicating denser and healthier vegetation. By calculating NDVI for multi-temporal Sentinel-2 scenes over the study period and taking the median composite, we derive the summer spatial distribution of NDVI for Shanghai. As an important indicator of urban greenness, NDVI is widely used in studies of land surface temperature and urban thermal environments [12]. The NDVI imagery produced in this study is then used to analyze the relationship between vegetation cover and land surface temperature.

2.5. Estimation of heat-island intensity

To assess the intensity of the urban heat island in summer, we calculated surface UHI intensity (SUHI) using the difference between mean LST in the urban core and that in suburban reference areas. Specifically, based on land use and administrative divisions, we designated the contiguous built-up area of central Shanghai as “urban,” and selected outlying areas dominated by agriculture and natural vegetation as the “suburban” reference. Using the processed LST raster, we computed the mean LST over the urban area and over the suburban reference area and took their difference [13]. A positive SUHI indicates the urban mean LST exceeds the suburban background (larger values mean stronger UHI); a negative or near-zero value indicates no obvious UHI. This provides a quantitative measure of average SUHI for subsequent analysis of its relationship with greenness.

2.6. Statistical analysis methods

After obtaining the spatial distributions of LST and NDVI and the SUHI metric, we quantified the NDVI–LST relationship at the district scale. For each administrative district in Shanghai, we extracted mean LST and mean NDVI by averaging pixel values within district polygons. We then applied Pearson correlation analysis to test for linear correlation between district-level mean NDVI and mean LST, reporting the correlation coefficient r and its significance under a 95% confidence level (α=0.05). A significant negative r indicates that districts with higher NDVI tend to have lower LST, providing initial evidence that greenness reduces surface temperature; a positive or non-significant r suggests no clear linear relationship.

DOI: 10.54254/2755-2721/2025.GL27816

We estimated β_0 (intercept) and β_1 (slope) via least squares, reported the coefficient of determination R^2 and the significance of coefficients to evaluate explanatory power and effect size. If the model passes significance testing ($p<0.05$), NDVI exerts a statistically significant linear influence on LST, with the sign of β_1 indicating directionality. By combining the Pearson correlation coefficient and an OLS regression model, we can quantitatively reveal the strength and linear pattern of the relationship between district-level greenness and land surface temperature (LST) across Shanghai. All statistical analyses were conducted in Python with the necessary significance and assumption checks to ensure robustness.

3. Results

3.1. Spatial distribution characteristics

Table 1. Lists district-level mean NDVI, LST, and SUHI for the summer of 2022 in Shanghai

	NDVI	LST (°C)	SUHI (°C)
Baoshan District	0.2865	46.7347	9.9759
Chongming District	0.5042	38.7555	1.9967
Fengxian District	0.4231	44.1738	7.4151
Jiading District	0.3331	45.0634	8.3046
Jinshan District	0.4441	45.9350	9.1762
Minhang District	0.3192	45.8211	9.0623
Nanhui (Pudong New area) District	0.3813	43.7198	6.9610
Pudong District	0.3234	44.8652	8.1064
Qingpu District	0.3574	41.8722	5.1134
City Center	0.2424	47.0661	10.3073
Songjiang District	0.3913	42.7788	6.0200

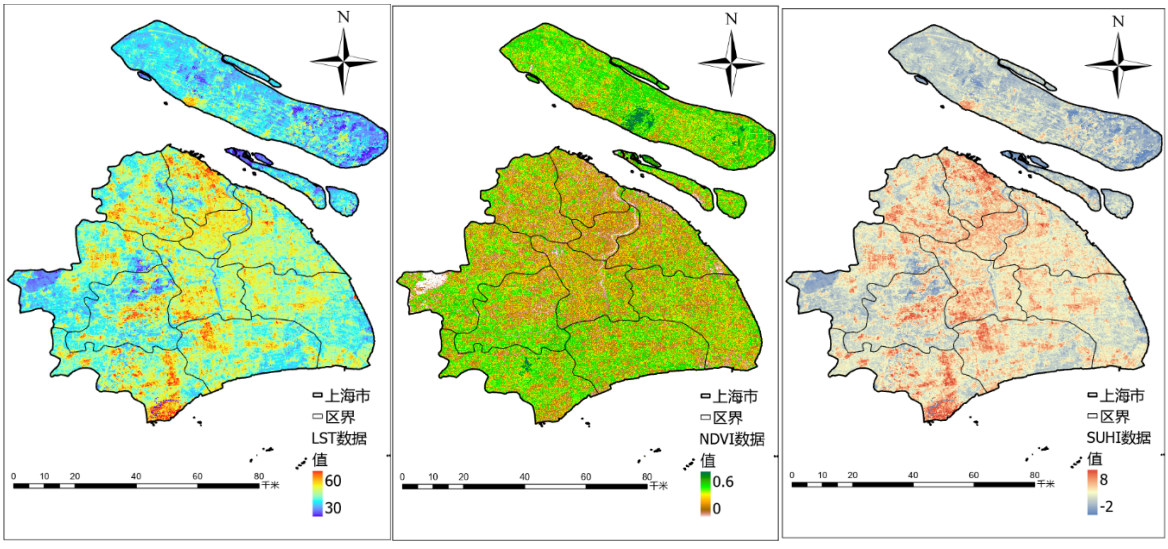

Figure 1. Spatial distribution maps of LST, NDVI, and Surface Urban Heat Island (SUHI) intensity in Shanghai (picture credit: original)

DOI: 10.54254/2755-2721/2025.GL27816

The mean NDVI across districts is 0.364 (SD 0.075), ranging from 0.242 to 0.504; mean LST is 44.3 °C (SD 2.4 °C), ranging from 38.8 to 47.1 °C; mean SUHI is 7.5 °C (SD 2.4 °C), ranging from 2.0 to 10.3 °C. Notably, Chongming has the highest NDVI ,0.504; and the lowest LST (~38.8 °C), whereas the City Center has the lowest NDVI (0.242) and the highest LST (47.1 °C), preliminarily indicating an inverse relationship between vegetation cover and surface temperature (Table 1) (Figure 1).

3.2. Correlation and regression analysis

To quantify relationships among NDVI, LST, and SUHI, we performed Pearson correlation and linear regression:

As shown in Figure 2 and 3, NDVI and LST exhibit a significant negative correlation (Pearson). The linear regression indicates that a 0.1 increase in NDVI is associated with a reduction of about 2.4 °C in district-mean LST, with the regression equation. NDVI is also clearly negatively correlated with SUHI (r = -0.732, p = 0.010). Since SUHI is essentially the increment of LST relative to the suburban background, the NDVI–SUHI trend closely mirrors the NDVI–LST relationship.

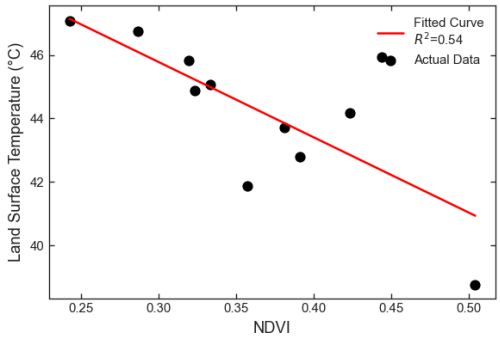

Figure 2. Relationship between NDVI and Land Surface Temperature (LST) in Shanghai (picture credit: original)

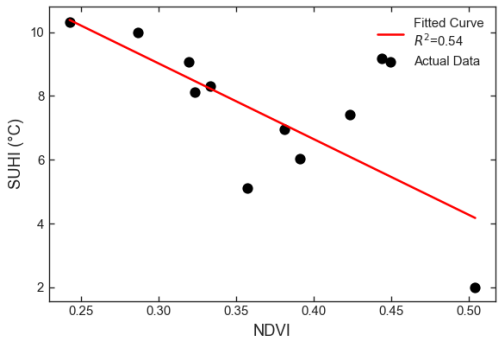

Figure 3. Relationship between NDVI and Surface Urban Heat Island (SUHI) intensity in Shanghai (picture credit: original)

DOI: 10.54254/2755-2721/2025.GL27816

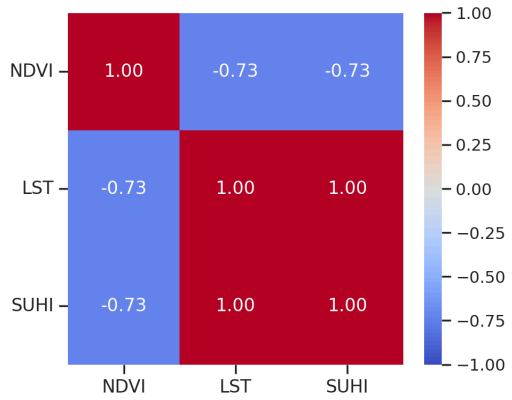

Figure 4. Correlation matrix of NDVI, LST, and SUHI

Figure 4 presents a correlation-matrix heat map for NDVI, LST, and SUHI: both NDVI–LST and NDVI–SUHI correlations are about −0.73 (blue) and significant; LST and SUHI are nearly perfectly positively correlated (r≈1.00, deep red), reflecting their high linear dependence. Overall, the analyses clearly show significant negative relationships between NDVI and both LST and SUHI: higher vegetation cover corresponds to lower surface temperatures and weaker heat-island intensity.

4. Discussion

4.1. The regulating role of vegetation on LST

Our results show a significant negative relationship between summer NDVI and LST in Shanghai—districts with higher vegetation cover tend to have lower LST, and vice versa—consistent with extensive prior literature [14]. Vegetation regulates surface temperature through multiple physical processes. When natural vegetation is replaced by impervious surfaces such as concrete and asphalt, evapotranspiration declines markedly while heat capacity and sensible heat flux increase, raising LST and forming urban heat islands [15]. In contrast, suburbs with abundant vegetation and water bodies divert more solar energy to evapotranspiration; vegetation-covered surfaces also have relatively higher albedo, leading to overall lower LST. This contrast in the distribution of vegetation versus impervious surfaces underlies the typical “hot core, cool periphery” pattern observed in Shanghai. Intensive human activities in the urban core—transportation, air-conditioning, etc.—emit considerable anthropogenic heat, exacerbating heat accumulation, especially at night.

Vegetation type and condition matter. High-density tree cover and forests, with higher leaf-area index and stronger transpiration, generally provide greater cooling than low grasses. Water bodies and vegetation blue-green spaces both help regulate LST: water cools via evaporation and heat capacity, while vegetation cools chiefly via transpiration and shading. Thus, the extent and configuration of blue-green spaces directly affect summer LST. Overall, increasing vegetation cover remains an effective strategy to reduce LST and mitigate UHI, offering scientific support for urban environmental management.

4.2. Causes of the heat island spatial pattern

Summer LST in Shanghai shows pronounced spatial variation: high temperatures are concentrated in the City Center (within the Inner Ring), while outlying districts are relatively cooler, forming a typical “heat-island–cool-island” pattern. More than half of the City Center area falls within high-

DOI: 10.54254/2755-2721/2025.GL27816

temperature zones, whereas roughly 30% of suburban areas belong to low-temperature zones. This "hot core, cool periphery" pattern reflects the canonical UHI phenomenon.

The drivers are closely tied to land-cover contrasts between the urban core and the suburbs. Impervious surfaces (e.g., concrete, asphalt) absorb and store solar energy by day and release it slowly at night; the scarcity of vegetation limits evapotranspiration-driven cooling, elevating LST in central districts [14]. By contrast, outlying areas with extensive vegetation and water redirect more solar energy to latent heat flux and often have higher albedo, yielding lower LST overall. Dense human activities in the core further amplify the UHI.

Numerous studies corroborate these land-cover controls in Shanghai: with increasing distance from the urban center, the fraction of impervious surfaces (buildings, roads) generally declines while vegetation cover rises, and LST tends to decrease accordingly [16, 17]. In other words, LST is positively associated with imperviousness and negatively associated with vegetation density [18]. Moreover, the marginal warming effect of adding impervious area is often larger than the marginal cooling from adding the same area of green space, explaining why modest greening may not fully offset heat accumulation in highly urbanized districts—the "push-up" effect of the built environment can exceed the "pull-down" effect of vegetation.

4.3. Planning and management implications

Findings highlight the critical role of vegetation in alleviating surface heat. The foremost planning recommendation is to substantially increase urban green space. Adequate greening reduces local LST via enhanced evapotranspiration, shading, and higher surface albedo. In practice, this entails creating and expanding multiple types of green spaces—new large urban parks, pocket parks, continuous green corridors along roads and waterways, and the promotion of rooftop and vertical greening—to raise citywide green volume [17]. More vegetation not only directly cools sun-exposed surfaces but also creates additional "cool-island" patches, mitigating overall UHI intensity.

Water bodies warrant emphasis due to their strong cooling and microclimate-regulating functions. Protecting and expanding water areas can lower surrounding thermal environments via evaporative cooling. Coordinated blue-green layouts help form a natural cooling network that counteracts the heat generated by high-density development.

Urban form also matters. A monocentric, high-density morphology can overly concentrate heat in the core. We recommend a polycentric, clustered spatial structure, distributing commercial centers and jobs more evenly to avoid excessive concentration in a single CBD and to diffuse heat structurally. Limiting the expansion of impervious surfaces is equally important: planning should cap impervious ratios, encourage permeable pavements and open green spaces, and reduce continuous large hard-paved areas in high-FAR redevelopment zones. Strengthening streetscape greening and increasing canopy cover can form continuous shade networks at the street scale and improve local microclimates.

4.4. Limitation and uncertainties

Despite demonstrating a significant negative NDVI–LST relationship in summer and elucidating the regulatory role of vegetation via spatial analysis, several limitations remain:

The first one is Temporal scope. This study focuses on summer daytime satellite data and thus mainly reflects daytime summer thermal conditions. Seasonal and diurnal variations were not examined; prior work shows that the cooling effect of vegetation varies by season, and NDVI–LST

DOI: 10.54254/2755-2721/2025.GL27816

relationships may weaken—or even become locally positive—in winter when deciduous vegetation is sparse. Broader seasonal and day–night analyses are warranted.

Secondly, relatively low Spatial resolution is also a limitation The 30 m Landsat pixel size captures overall urban patterns but may miss finer-scale features. Our results apply primarily at scales of tens of meters and above; block- and street-level thermal heterogeneity remains uncertain and could be examined with higher-resolution data or in-situ monitoring.

5. Conclusion

Using multi-source remote-sensing data, this study quantifies the relationship between urban vegetation cover and the surface thermal environment. In summer Shanghai, NDVI and LST are significantly negatively correlated; increasing vegetation effectively reduces LST and mitigates UHI. Building on this, we clarify the pivotal role of greening in UHI mitigation and answer the core question of where and by how much vegetation delivers effective cooling.

For practice, substantially expanding green space is the most direct and effective strategy. Cities should increase large parks and community green areas, build continuous green corridors along roads and rivers, and promote rooftop/vertical greening to enhance overall vegetation cover. Blue-green coordination and the protection/expansion of water bodies can further alleviate high-temperature conditions via evaporative cooling. Optimizing urban spatial structure toward polycentric layouts and strictly controlling impervious expansion are also essential. Implemented together, these measures can create a more complete natural cooling network, significantly enhancing urban climate resilience and thermal comfort.

Limitations suggest several directions for future work: incorporate other seasons and nighttime data to assess temporal variability; use higher-resolution imagery or fine-scale monitoring to capture micro-scale heterogeneity; and integrate socioeconomic and demographic data to evaluate differential heat exposure and green-space access across communities, thereby supporting more equitable climate-adaptation strategies. In sum, sustained cross-seasonal, cross-scale, and cross-disciplinary research on urban thermal environments will better guide green-infrastructure planning and UHI mitigation.

References

[1] Gsnvksn, S., et al. (2017). Urban heat island (UHI) influence on secondary pollutant formation in a tropical humid environment. Journal of the Air & Waste Management Association.
[2] U.S. Environmental Protection Agency. (2017). Heat island impacts. EPA.
[3] Gunawardena, K. R., et al. (2017). The influence of urban vegetation on urban heat island. Journal of Applied Meteorology & Climatology.
[4] Zhang, Z., et al. (2023). Cooling efficacy of trees and urban background climate. Nature Communications.
[5] Jiang, Z., et al. (2006). Analysis of NDVI for vegetation fraction retrieval. Remote Sensing of Environment.
[6] Zhang, J., & Wang, Y. (2008). SUHI spatial extent and urban factors. Sensors.
[7] Lin, N., et al. (2023). Urban vegetation extraction from high-resolution imagery via deep learning. Remote Sensing.
[8] Li, W., et al. (2018). GWR analysis of factors related to SUHI. Remote Sensing.
[9] Sun, T., et al. (2025). Coupling effect of urban features on LST. Urban Forestry & Urban Greening.
[10] Gorelick, N., et al. (2017). Google Earth Engine: Planetary-scale geospatial analysis for everyone. Remote Sensing of Environment.
[11] Ermida, S. L., et al. (2020). Google Earth Engine open-source code for land surface temperature estimation from the Landsat series. Remote Sensing, 12(9), 1471.
[12] Wang, M., Meng, H., Bai, Y., Su, J., Sha, C., & Zhang, M. (2013). Relationships between land-use spatial pattern and land-surface temperature in Shanghai (in Chinese, English abstract). Ecology and Environmental Sciences, 22(2), 343–350.

DOI: 10.54254/2755-2721/2025.GL27816

[13] Li, Y., Yin, K., Zhou, H., Wang, X., & Hu, D. (2016). Progress in urban heat-island monitoring by remote sensing (in Chinese, English abstract). Progress in Geography, 35(9), 1062–1074.
[14] Chao, Z., Wang, L., Che, M., & Hou, S. (2020). Effects of different urbanization levels on land surface temperature change: Taking Tokyo and Shanghai for example. Remote Sensing, 12(12), 2022.
[15] Li, B., Wang, H., Qin, M., & Zhang, P. (2017). Comparative study on the correlations between NDVI, NDMI and LST. Progress in Geography, 36(5), 585–596.
[16] Wang, H., Zhang, Y., Tsou, J. Y., & Li, Y. (2017). Surface urban heat island analysis of Shanghai (China) based on the change of land use and land cover. Sustainability, 9(9), 1538.
[17] Yang, J., & Bou-Zeid, E. (2019). Scale dependence of the benefits and efficiency of green and cool roofs. Landscape and Urban Planning, 185, 127–140.
[18] Zhang, H., Li, T.-T., & Han, J.-J. (2020). Quantifying the relationship between land use features and intra-surface urban heat island effect: Study on downtown Shanghai. Applied Geography, 125, 102305.